HardwareX 14 (2023) e00428

Contents lists available at ScienceDirect

HardwareX

journal homepage: www.elsevier.com/locate/ohx

Low-cost acoustic force trap in a microfluidic channel

Vi-hung Tsan, Daniel Fan, Sabina Caneva, Carlas S. Smith, Gerard J. Verbiest *

Faculty of Mechanical, Materials, and Maritime Engineering, Technische Universiteit Delft, Delft 2628CD, The Netherlands

ARTICLE INFO

Article history:

Keyword:
Acoustic trapping
Acoustic force spectroscopy
Acoustophoretic
Microfluidics
Low-cost

ABSTRACT

A low-cost glass-based microfluidic flow cell with a piezo actuator is built using off-the-shelf parts (total cost €9 per device) to apply acoustophoretic force on polystyrene micro-beads. The main challenge in the fabrication of these devices was to ensure their leak tightness, which we solved using double-sided tape and nail polish. Beads with 1.5 μm diameter flowing in a 100 μm deep channel were trapped at 7.5 MHz using a 23.7 peak-to-peak voltage (V_{pp}) sinusoidal input. The trap located at 50 ± 0.1 μm depth was measured to have a stiffness of approximately 0.6 pN/μm. With this simple device we can trap and control the axial position of micrometer scale objects, which allows for the manipulation of beads and cells. We intend to use the device for force spectroscopy on micro-bead tethered DNA. This can be combined with super-resolution imaging techniques to study mechanics and binding of protein structures along a DNA strand as a function of induced tension.

Specifications table

Hardware name	Microfluidic acoustic force trap
Subject area	• Engineering and material science • Biological sciences (e.g. microbiology and biochemistry) • Educational tools and open source alternatives to existing infrastructure • General
Hardware type	• Imaging tools • Measuring physical properties and in-lab sensors • Mechanical engineering and materials science
Closest commercial analog	Lumicks z-Movi [1] or uFluidix custom chip [2]
Open source license	Copyright 2022 under the GNU General Public License (GPL).

(*continued on next page*)

* Corresponding author.
E-mail addresses: c.s.smith@tudelft.nl (C.S. Smith), g.j.verbiest@tudelft.nl (G.J. Verbiest).

https://doi.org/10.1016/j.ohx.2023.e00428
2468-0672/

* (*continued*)

Hardware name	Microfluidic acoustic force trap
	This hardware is free; you can redistribute it and/or modify it under the terms of the GNU General Public License as published by the Free Software Foundation; either version 2 of the License, or any later version. This hardware is distributed in the hope that it will be useful, but WITHOUT ANY WARRANTY; without even the implied warranty of MERCHANTABILITY or FITNESS FOR A PARTICULAR PURPOSE. See the GNU General Public License for more details. You should have received a copy of the GNU General Public License along with this article; if not, write to the Free Software Foundation, Inc., 51 Franklin St, Fifth Floor, Boston, MA 02110–1301 USA
Cost of hardware	9–230 EUR
Source file repository	https://figshare.com/s/dd6a9df122444dfbc496

1. Hardware in context

Microfluidic tweezers are a versatile technology widely used for research in biotechnology, medicine and chemistry [3]. The trapping and manipulation of micrometer-sized objects within microfluidic channels is especially relevant for cell studies, molecular biology, biotechnology, and medicine [4]. In fact, the trapping of microbeads is becoming an indispensable tool to study structural and mechano-chemical properties of proteins and DNA [5]. Insight into these properties may even lead to the development of medicine for currently incurable diseases.

Well-known manipulation platforms utilize optical tweezers, magnetic tweezers or atomic force microscopy. Optical tweezers require complex optics and deliver high output power. The high power output has been reported to damage cells during trapping experiments [6]. The use of these single-molecule manipulations is therefore restricted to specialized biolabs. All the aforementioned platforms require specialized expertise for their construction and operation and offer limited throughput [7,8].

A particle manipulation technique using acoustic waves to exert acoustophoretic forces on microbeads may provide a solution. Compared with other micro-manipulation methods [9]1011, the acoustic tweezer is relatively low-cost and less demanding in terms of hardware. Acoustic tweezers also avoid common micro-object trapping issues such as local heating (optical trapping), charge screening in salty solutions (electrical trapping), customized beads (magnetic trapping), low throughput (mechanical trapping[12]), and limited control (hydrodynamic trapping). In particular, acoustic tweezers allow for a high number of particles to be trapped simultaneously for high-throughput measurements and is applicable to a large range of particles [13]. Although acoustic traps have a lower spatial resolution than other trapping platforms, they can still provide performance similar to magnetic traps. The high throughput capability is a key advantage over other manipulation platforms since stochastic models describe most biological processes [14]15. This tool can therefore provide scientists with statistically significant data time-efficiently.

Acoustic trapping, acoustic levitation, and acoustic force manipulation in general have been widely studied in air, using near-field, far-field, standing-wave, and single-beam modalities. This can then be used to study liquid droplet physics, rotate and translate objects, and merge liquid objects [16]. For example, these devices can be used for contact-less transportation of fragile silicon wafers [17]. This can lead to a considerable reduction in the price of microchips found in nearly all devices. Application of these methods in liquid environments and scaled down to micrometer dimensions allows the manipulation of cells and biomolecules. For example, using surface acoustic waves, acoustic forces can be used to manipulate cells in 3D (albeit at the expense of complicated device fabrication) [18]. The acoustic tweezer can also be used to sort microparticles based on size. This ability allows it to be used to filter out bacteria or dust particles from water [19].

For acoustic tweezers to be used in, for example acoustic force spectroscopy, the trapping device needs to able to deliver up to 120 pN force to overstretch DNA and unfold proteins [20]2114. This should be induced on a DNA strand with a length of around 10 μm due to the limited range of 3D particle tracking methods [22]. In addition, the attached bead to the DNA should have a diameter of 4.5 μm based on a comparable device in literature [5]. Note that the typical size of beads used in acoustic trapping experiments ranges in diameter from 1 to 20 μm [23]. For the device to be compatible with current experimental techniques to study biological processes at the sub-micrometer scale, we require optical access. Therefore, the design should use standard glass cover slips with a thickness of 170 μm. This requirement ensures that this device is compatible with most microscopes.

All the design requirements are summarized as follows:

- Low-cost using off-the-shelf parts.
- Trap micro-beads with a diameter between 1 and 20 μm.
- Trap multiple beads simultaneously.

- A trapping force equivalent to ∼120 pN for a 10 μm DNA strand attached to a 4.5 μm polystyrene bead.

Multiple designs using acoustic traps have been realized, including surface acoustic waves, travelling waves, and acoustic streaming [24]. However, we focus on one of the simplest designs: a layered resonator, schematically shown in Fig. 1, which uses a bulk acoustic standing wave to levitate micro-objects in the middle of a microfluidic channel [25]5. We can study the interactions between neighbouring objects by trapping objects at the focal plane of the imaging device. Furthermore, by tethering DNA strands to the glass slide and micro-beads at the other end of the DNA and trapping those beads, we can perform acoustic force spectroscopy on DNA strands [5].

2. Hardware description

We present a simple, easy-to-build, and low-cost microfluidic device with a piezo actuator based on [5]. As far as the authors are aware, the closest commercial equivalents are an integrated system specifically made for measuring cell avidity [1] and a custom-made system that becomes cost-effective only for bulk orders [2] and therefore not suitable for rapid prototyping. The device we present is:

- Suitable for biological experiments involving bead trapping and stretching of tethered biomolecules such as DNA.
- Re-usable for biological experiments as the glass slides are easily cleaned and (re-) functionalized.
- Suitable for (bio-) physics experiments to study the interactions between particles close to each other.
- Compatible with super-resolution imaging due to the visual access through standard glass cover slips.
- Suitable for high-throughput experiments as multiple beads can be trapped at the same time.
- Suitable for experiments in education to explain acoustic forces.
- Cheaper than commercial devices.

To check the design requirements, we simulated the acoustic pressure field in the device shown in Fig. 1 using COMSOL Multiphysics 5.6 (see design files). We verified the results using calculations based on an equivalent circuit model [26] that provides the required acoustic frequency to trap beads in the microfluidic device. This acoustic frequency is determined by the device geometry and speed of sound. The fundamental frequency f_0 corresponds to the longest wavelength standing wave in the microfluidic channel. Given $h = 100\mu$m, the height of the microfluidic channel, and v the speed of sound in water ($\approx$ 1480 m/s), we find $f_0 =$ 7.4 MHz. We selected a piezo disc transducer based on the highest off-the-shelf resonance frequency available. Then we selected the smallest channel height where the calculated f_0 is below the rating of the piezo disc.

The other materials in the device were chosen to ensure a minimal amount of acoustic damping. Typically, customized microfluidic devices are made from polymers such as polydimethylsiloxane (PDMS), which are easier to mold into channels. However, since we require high Q-factors to avoid damping of acoustic forces, we chose a glass substrate and glass matching layer. At first, we tried to fabricate a microchannel in the glass substrate via laser ablation using a fs-laser cutter, followed by bonding the glass cover slip via dehydration condensation [27]. However, while the laser-cut channel profile was accepTable (100 μm deep and 200 μm wide), the slag at the edges of the channel bulged out slightly by approximately 3–5 μm. This bump prevented strong glass-glass bonding as the two surfaces were not sufficiently flat. Consequently, these devices were suffering from severe leakage problems. Therefore, we fabricate the microfluidic channel in the final design using two strips of double-sided tape. In this case, care must be taken to prevent air bubbles in the adhesion surfaces by pressing gently but firmly down using a plastic pipette. The edges can then be sealed using epoxy glue or nail polish.

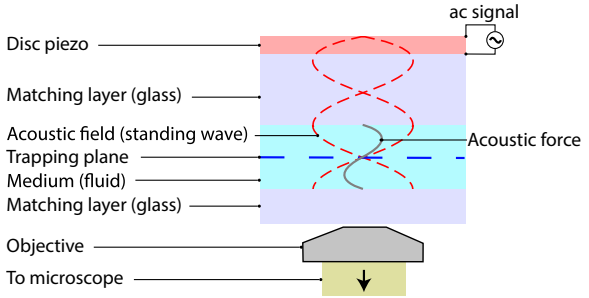

Fig. 1. Concept of acoustic tweezers. Sound waves are generated by disc piezo actuated with an ac signal from a voltage source. At the fundamental frequency the resulting acoustic field is a standing wave, with a pressure node appearing in the middle of the fluid channel. Beads and other micro-objects are trapped at this nodal plane, hence trapping plane, due to the scattering of acoustic waves. The trapped objects can be observed through an objective connected to a microscope.

Design filename	File type	Open source license	Location of the file
model_with_piezo.mph	COMSOL simulaion	GNU	https://figshare.com/s/dd6a9df122444dfbc496
model_with_piezo_tape.mph	COMSOL simulation	GNU	https://figshare.com/s/dd6a9df122444dfbc496

3. Design files summary

A finite element model (COMSOL) used to simulate the acoustic pressure is provided for purposes of design modification. It models the structure depicted in Fig. 2. Since the device is made from off-the-shelf components, only a sketch is provided along with build instructions.

4. Bill of materials summary

The total cost of the device (not including ac voltage source and microscope) is approximately €9. For minimum order amounts, the total cost is approximately €230. This does not include equipment necessary for fabrication: soldering iron, solder, drill with a bit suitable for glass, ultrasonic bath, pipette tip, scalpel, toothpick, gloves, nail polish, and solvents for cleaning.

5. Build instructions

Fig. 3 shows photos corresponding to each step in the build instructions. All item numbers refer to Fig. 2.

(a) Drill two holes through a glass slide (item 6) roughly centered and roughly 40 mm apart. A Dremel-type drilling tool with a 4 mm diameter drill bit suitable for glass can be used at low rpm and light pressure.
(b) Clean glass slide (item 6) and cover slip (item 8) using acetone immersion combined with ultrasonic cleaning for 5 min, then isopropanol immersion with ultrasonic cleaning for 5 min, followed by a thorough rinse in deionized water and drying under an air-gun.
(c) Place the glass slide (item 6) on a clean, flat surface and tape it down along the two long edges with double-sided tape (item 7), leaving a 2 mm gap between the tapes and down the middle of the glass slide. Make sure the tape is flat.
(d) Carefully place the cover slip (item 6) on top of the two double-sided tapes.
(e) Use a plastic pipette tip to gently press the cover slip down into the tape so that it is flat. Interface colour darkening as the cover slip is pressed indicates good contact of the cover slip with the tape. Therefore, press all along the edges of the microchannel.

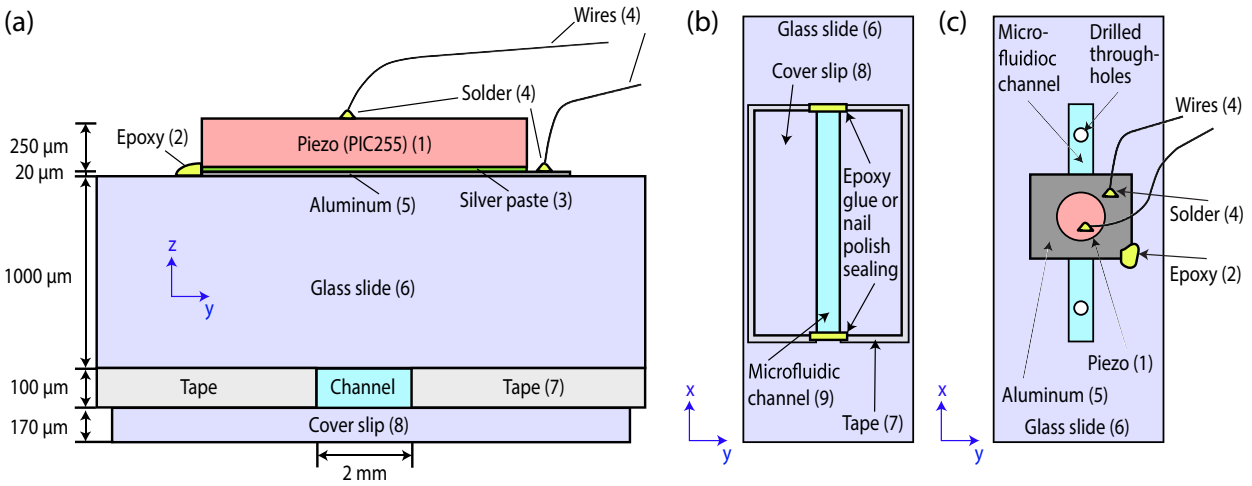

Fig. 2. Schematic of the device with side view along the length of the microchannel (a), bottom (b) and top-down view (c). Numbers (1)-(8) correspond to the designator specified in Section 5.

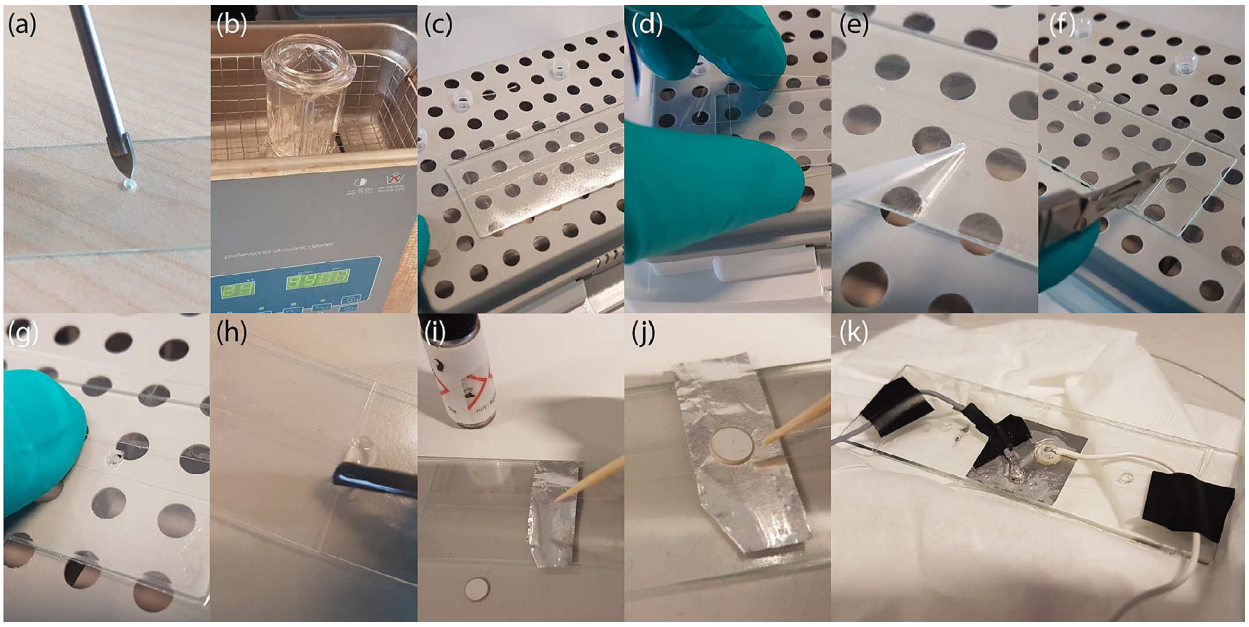

Fig. 3. Fabrication procedure as outlined in Section 6.

(f) Use a scalpel to remove the excess double-sided tape.
(g) If there are through-holes, ensure the double-sided tape does not cover them.
(h) Once the cover slip is placed over the microchannel, the edges can be sealed using epoxy glue or nail polish.
(i) Cut a thin strip of aluminium foil (item 5) of approximately 5 mm x 20 mm. Place on the glass slide over the microchannel. Use a toothpick to place a droplet of conductive silver paste (item 3) in the center of the aluminium foil over the microchannel. Place the piezo disc (item 1) on top of the silver paste droplet and press down.
(j) Using another toothpick, cover the edges of the foil/piezo disc sitting on top of the glass slide with epoxy glue (item 2). Wait for it to cure (approximately 1 h).
(k) Once cured, solder one wire (item 4) onto the top of the piezo disc and one wire (item 4) onto the excess aluminium foil. The top and bottom of the piezo disc should now be electrically contacted by wires. Use tape to ensure the wires are mechanically stable.

- Safety: be careful when using the scalpel and soldering iron. Ensure ventilation when using epoxy glue and silver paste.

6. Operation instructions

- Flush the microchannel with deionized water using a pipette at one end and tissue at the other end or via the through-holes.
- Connect the wires to the amplifier (Analog Devices ADA4870) and connect the amplifier to the signal generator (RS pro RSDG 830) and power supply (Delta electronika E018-0.6D) as shown in Fig. 4.
- Fill the channel with 1.5 µm diameter polystyrene microbeads (Poly sciences Fluoresbrite YG carboxylate, or other micro-objects) suspended in deionized water.
- Place the chip on an inverted microscope. The device is now ready for imaging and trapping of micro-objects using acoustophoresis. For example, turn the signal generator on to generate a sinusoidal with a frequency of 7.5 MHz and adjust the amplitude by using this signal generator, whose amplitude will be amplified approximately 2.7 times by the amplifier to output the required V_{pp}. For our device, we did not observe trapping when shifting the frequency by $\pm$0.1 MHz away from the 7.5 MHz trapping frequency or when V_{pp} was below 8 V. The beads should now be trapped at the trapping plane, which can be observed through the microscope by adjusting the excitation intensity level and camera exposure time. In this paper the Nikon Eclipse TS2R inverted microscope with a water immersion objective (NA = 1.1 and 60x magnification) was used for the derivation of the calibration curve and trapping experiments. The camera pixel size is 0.126 µm per pixel with an array size of 4908 by 3264 pixels. The image acquisition settings are: 50 frames per second, exposure time of 500 µs, a light source with a wavelength of 470 nm and the light intensity is set with 64 times analog gain and ten manual turns on the intensity knob.
- Safety: ensure electrical connections are well made and not touching each other.

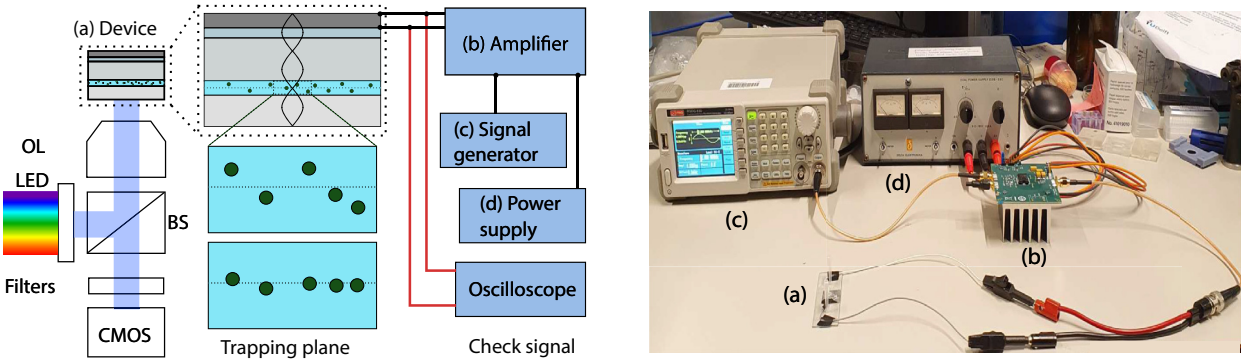

Fig. 4. The left image schematically depicts the setup used for acoustic trapping experiments. The movement of the beads is imaged through an objective lens (OL) with filtered light from a light-emitting diode (LED) source that passes through a beam splitter (BS), and the reflected light from the beads is processed with a digital camera (CMOS). The chip (a) is connected to the output of the amplifier (b), which is connected to the signal generator (c) and power supply (d). An oscilloscope can be connected in parallel to the chip to check the input signal. The right image is a photo of the actual setup, where (a) represents the device, (b) amplifier (Analog Devices ADA4870), (c) signal generator (RS pro RSDG 830) and (d) power supply (Delta electronics E018-0.6D).

7. Validation and Characterization

The trap stiffness of the fundamental frequency can be derived from the FEM model by calculating the acoustic radiation force profile in the middle of the channel. We find this profile by computing the force on ten evenly spaced 1.5 μm polystyrene beads placed along the z-axis (Fig. 2a) in the microfluidic channel. We use ten beads to sample the sinusoidal acoustic force profile with a sampling rate ten times its frequency [28] while having negligible interaction between the beads themselves. We fit a sine wave to these ten data points to extract the acoustic radiation force profile shown in Fig. 5a for varying peak-to-peak actuation voltages V_{pp}. By taking the derivative of fitted acoustic radiation force profiles at the middle of the channel (z = 50 μm) with respect to z, we estimate the trap stiffness for the fundamental frequency. We perform these simulations with and without presence of a glue layer between the aluminium and glass slide (item 5 and 6 in Table 1) as shown in Fig. 2. By repeating this procedure for all relevant V_{pp} values, we obtain the trap stiffness curves shown in Fig. 5b. The glue layer between the aluminium layer and glass slide is assumed to have a thickness of 20 μm, which is around the same thickness as the aluminium layer. The material properties of the epoxy layer in the simulation are: E = 3.45 GPa, ν = 0.321, ρ = 1.44 kg/m^3 [29].

The force on a DNA strand with a length of 10 μm can be derived from the trap stiffness by observing that the derivative at the center of the channel (z = 50 μm) in Fig. 5c is roughly equal to the derivative at z = 0 μm and z = 100 μm. In addition, the acoustic radiation force can be approximated to be linear close to a node. Therefore, the force on a DNA strand is the length of the strand multiplied by the trap stiffness for the fundamental frequency. For our device, we find a simulated trap stiffness of 0.9 (2.4) pN/μm for 23.7 V_{pp} at 7.41 MHz with (without) glue. This value times the length of the DNA becomes 9 pN and 24 pN, respectively. These values are a good approximation of the actual force experienced at 10 μm away from the bottom glass layer (at z = 0 μm) or top glass layer (at z = 100 μm).

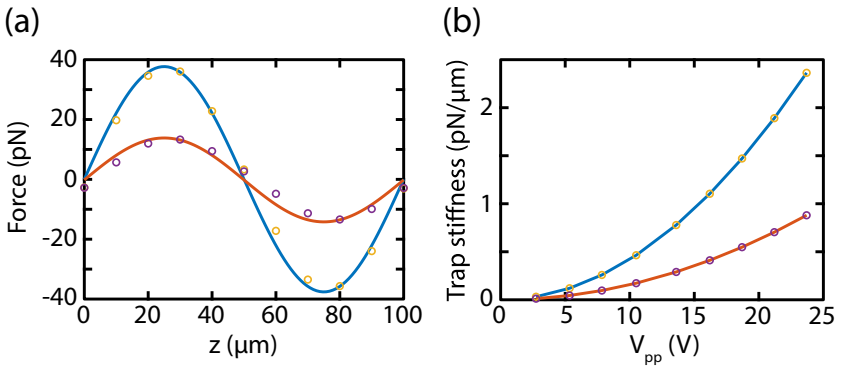

Fig. 5. Procedure to extract the trap stiffness from simulation. (a) Extracted acoustic radiation force on the given bead position at excitation frequency of 7.41 MHz and an amplitude of 23.7 V_{pp} for the simulation with (purple/red) and without (yellow/blue) glue. The continuous red and blue lines represent the corresponding fits of the force with a sine function. (b) Extracted trap stiffness as a function of V_{pp} at 7.41 MHz from the simulation with (purple/red) and without (yellow/blue) glue.

Table 1
Materials needed to build the chip (euro 8.79 per chip).

Designator	Component	Number	Cost per unit currency	Total cost currency	Source of materials	Material type
1	Piezo disc PRYY + 0398	1	€8	€8 (minimum order €80)	Physik Instrumente (PI) GmbH & Co. KGhttps://www.physikinstrumente.store/eu/pryy-0398/?c=65670	Ceramic
2	Epoxy glue	0.1 gram	€11.49 per 30 gram	€0.04 (minimum orde €11.49)	Gammahttps://www.gamma.nl/assortiment/super-epoxy-30-gram/p/B432512	Polymer
3	Silver conductive paste	0.05 gram	€19.2 per 3 gram	€0.32 (minimum order €19.2)	Farnellhttps://nl.farnell.com/electrolube/scp03b/paint-conductive-scp-silver-3g/dp/725614?CMP=grhb-commerceconnect	Metal
4	Wires	30 cm	€0.21 per meter	€0.06 (minimum order €21)	RShttps://nl.rs-online.com/web/p/hook-up-wire/1805914	Metal, polymer
5	Aluminium foil	1 cm^2	€0.08 per meter	€0.08 (minimum order €1.39)	Actionhttps://www.action.com/nl-nl/p/dumil-aluminiumfolie-/	Metal
6	Glass microscope slide 631-1552 (76x26x1 mm)	1	€0.10	€0.10 (minimum order €5)	VWRhttps://nl.vwr.com/store/product/564378/objectglaasjes#order	Inorganic
7	Scotch 3 M double-sided tape 12 mm wide, 0.1 mm thick	20 cm	€2.95 per 6.3 meters	€0.10 (minimum order €2.95)	https://www.123inkt.nl/3M-Scotch-665-dubbelzijdig-tape-12-mm-x-33-m-6651233-i24276-t62000.html	Polymer
8	Glass cover slip #1.5 thickness 631-0853 (24 × 60 mm)	1	€0.09	€0.09 (minimum order €86.5)	VWRhttps://nl.vwr.com/store/catalog/product.jsp?catalog_number=631-0853	Inorganic

To experimentally validate the model, we first need to obtain a calibration of the true axial position of the microbeads with respect to the focal plane of the objective. We obtain this calibration curve by fixing Fluoresbrite YG carboxylate 1.5 µm polystyrene beads in 0.1 w/v % agarose solution and then scan the axial position of the focal plane through a bead. For each different axial position, we record an image with the camera (Fig. 6a). The camera had the following settings: exposure time of 1 ms, 470 nm wavelength light source, 64 analog gain light intensity and turning 30 times the manual light intensity knob. Then, we use a peak detecting algorithm [30] to detect bead locations in the recorded images (Fig. 6b). When the location of a bead is known, the image is cropped further to contain a single bead (Fig. 6c). The intensity profile of each bead image is normalized with its maximum value, and then fitted with a 2D Gaussian. The set of images obtained for different focal planes could also be analysed using holographic image reconstruction algorithms [31,32]. The 2D Gaussian fit uses nonlinear quadratic optimization to fit the 2D Gaussian function [33] to the intensity profile of the bead. This function reads as:

$$f(x,y) = Ae^{-\left(\frac{(x-x_0)^2}{2\sigma_x^2}+\frac{(y-y_0)^2}{2\sigma_y^2}\right)} + B, \tag{1}$$

where A represents the normalized amplitude of the bead intensity profile with a value between 0 and 1, (x_0, y_0) represents the center coordinate of the bead in micrometers, σ_x and σ_y represents the standard deviation of x and y in micrometers, respectively and thus is a measure for the bead radius. The parameter B represents the background term, which is set to zero as this resulted in the lowest variance in the calibration curve. The squared norm of the residual for the fit and the absolute

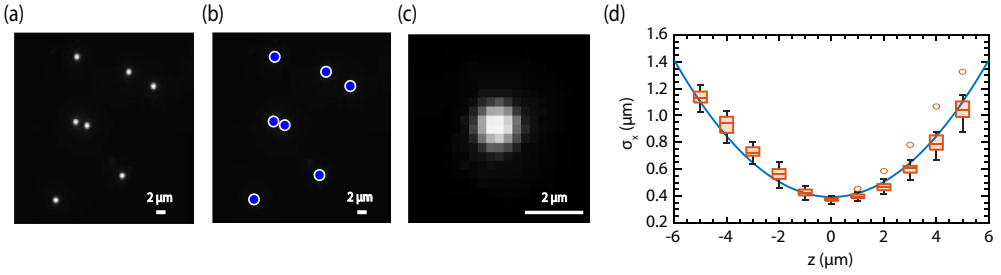

Fig. 6. Image processing procedure (a)-(c) represents a step-by-step procedure to obtain the calibration curve. (a) The original frame containing 1.5 µm beads in agarose for calibration, (b) detected beads in a 2D plane marked by blue circles, and (c) cropped image around a single bead which is fitted to Eq. 1. (d) The extracted width σ_x of the beads for different focal positions z. Error bars indicate the uncertainty, circles represent outliers, and the continuous blue line is the calibration curve (see Eq. 2).

difference between σ_x and σ_y needs to be smaller than a given threshold to filter out overlapping beads or beads that are excessively distorted due to planar motion, after which only σ_x is used. By applying this procedure to the sample with fixed beads for different focal planes obtained by manual adjustment of the microscope focus dial, we obtain the calibration curve as shown in Fig. 6d. The calibration curve is a fourth-order polynomial in z and is fitted to the medians of σ_x in a range of z from -5 to 5 μm as shown in Fig. 6d. The obtained fit has a R^2-value above 0.8 (R^2 = 0.86) and the resulting equation is:

$$\sigma_x = 2.69 \cdot 10^{-9} z^4 + 0.028 z^2 + 0.39. \tag{2}$$

We then placed the device in an inverted microscope (Nikon) and injected 1.5 μm polystyrene beads suspended in deionized water at a concentration of $\sim 2 \cdot 10^7$ beads/mL into the microfluidic channel. Low concentrations of beads are required to reduce the interaction between the beads that attract each other [34] and to avoid overlapping beads for the image processing. Videos of the suspended beads being trapped were recorded at a frame rate of 50 frames per second, exposure time of 500 μs, a light source with a wavelength of 470 nm and 64 times analog gain, and ten manual turns on the intensity knob to regulate the light source intensity. This ensures that the bead intensities were not saturated. Slightly different lighting conditions than in the calibration were used here for the experiment because of the low signal-to-noise-ratio of the calibration sample due to photo-bleaching. In order to deal with different lightning conditions the mean is subtracted and the intensity profiles of each bead is normalized with its maximum value [35] [36].

By following the same image processing procedure and filter settings as for the calibration but now by using a video captured during the trapping and the focal plane fixed at the trapping plane, we obtain values of σ_x for the trapped beads within a user-defined region of interest. We apply the calibration curve (Eq. 2) to these σ_x values (in μm) to obtain the distance δz from the focal plane. The absolute δz value is used since the calibration curve is symmetric, and only the distance between the bead and the focal plane can be calculated. However, since we are only interested in the trapping stiffness, this does not matter, and the absolute value of δz is sufficient. The obtained δz values are then mirrored about the $\delta z = 0$ μm axis to obtain a normal distribution (Fig. 7a). Hereafter, we extract the variance $var(z)$ of the distribution in δz by fitting a Gaussian to it.

The equipartition theory allows us to extract the acoustic trap stiffness using only $var(z)$. This theory depends on the frame rate of the image acquisition device, but will saturate to a fixed value, as shown by Pesce et al. [37] and Gerspach et al. [12]. Gerspach et al. described that the saturation value could be used to determine the trapping stiffness, which will make the equipartition theory independent of the frame rate of the capturing device. For one coordinate, the saturated equipartition theory value is given by [37]:

$$var(z) = \frac{2k_B T}{k_z} \tag{3}$$

Where $var(z)$ represents the variance in the axial position z, k_B represents the Boltzmann constant, T is the absolute temperature in Kelvin, and k_z is the stiffness of the trap in the axial direction z in N/m. As the experiment was done in a temperature controlled lab environment of 293.15 K, we find a trapping stiffness for 23.7 V_{pp} of 0.6 pN/μm. We extracted the trapping stiffness for different V_{pp} values as shown in Fig. 7b.

From the results shown in Fig. 7b, we were able to reach a trap stiffness of approximately 0.6 pN/μm at 23.7 V_{pp} for 1.5 μm polystyrene beads. The trap was located at 50 μm depth in the channel. Varying the frequency slightly away from 7.5 MHz caused the trap to disappear. Although the target stiffness was reached, there is still some discrepancy between simulated trap stiffness and experimentally obtained values, see Fig. 7b. We attribute this to the fact that the glueing layers

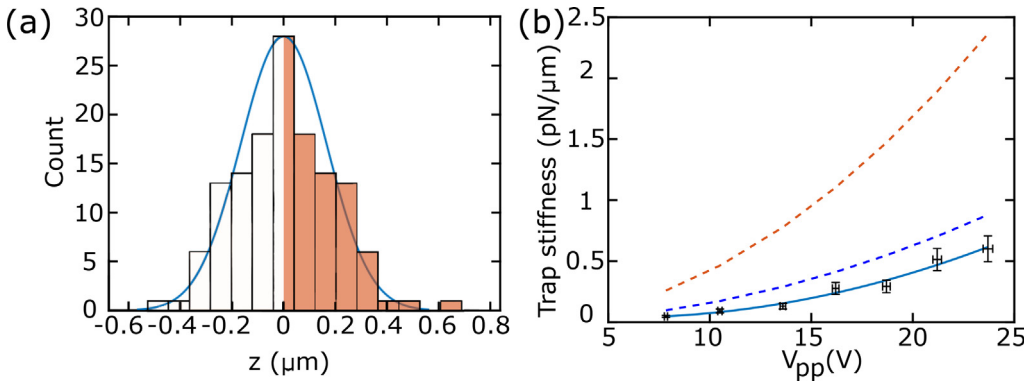

Fig. 7. (a) Example of histogram obtained with the image processing procedure and the calibration curve for trapping experiment at 7.5 MHz and 18.7 V_{pp} with z-coordinate representing the distance away from the trap/focal plane. The hollow side of the histogram represents the mirrored data since in the measurement only absolute values are recorded. The blue line is a least squares 1D Gaussian fit to the midpoint on top of each histogram (b) experimentally obtained trap stiffness (solid blue line) for different V_{pp}. The error bars represent the uncertainty in the experimental results and the blue solid line is a second order polynomial fit to the experimental data. For comparison, we show the dashed blue line and dashed red line representing the simulation result with and without glue (glue thickness of 20 μm).

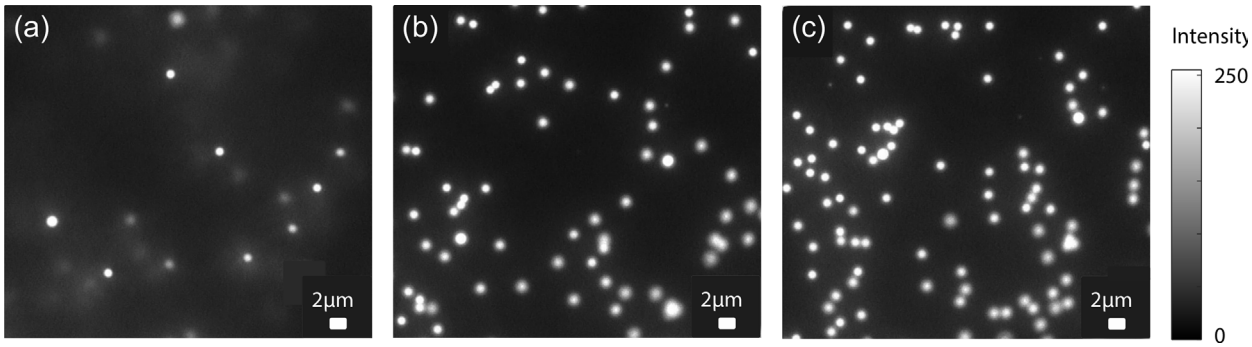

Fig. 8. (a) Beads image without actuation of piezo. (b) Bead trapping right after actuation of piezo. (c) Bead trapping after 9.6 s of actuation.

between piezo, aluminium foil, glass, and double-sided tape were not included in the finite element model. Air bubbles which become trapped at the tape-glass interfaces can form during fabrication, lowering the overall stiffness of the device. Further, operating the piezo at high input voltages can cause heating of the device, which in turn affects the mechanical properties of the glueing layers.

A video of the bead being trapped is included in the online repository. We extracted frames from this video to show the process of trapping (see Fig. 8). Initially, the beads suspended in a fluid are randomly distributed, as can be seen from the varying sizes in Fig. 8a. Once the trap is turned on (Fig. 8b), the beads move and stay at the focal plane. After some time, neighbouring beads start interacting with each other (Fig. 8c) and seem to cluster. The presented device and analysis method could form the experimental basis to study and quantify this interaction.

If we assume that the sinusoidal acoustic pressure field is roughly linear close to a node, then for a 10 μm DNA strand tethered to a 1.5 μm bead, the maximum force experienced is 6 pN. Since the acoustic radiation force on an object scales with its volume [5] and the gravitational and buoyancy forces are cancelled, we expect for a 4.5 μm bead (which has a three times larger diameter than a 1.5 μm bead) a $3^3 = 27$ times increase in maximum force. This would thus result in a force of 162 pN.

7.1. Conclusion & outlook

Some future suggestions to improve trap stiffness include using laser-cut channels with the channel edges ground down to achieve a flat glass surface suitable for glass-to-glass bonding. However, this might increase fabrication costs and require specialized tools. Purchasing piezo discs with wrap-around electrodes would help avoid too much glue on the top of the glass slide, but again with a matching cost increase.

In summary, we have fabricated a low-cost acoustic force microfluidic device suitable for trapping polystyrene beads to study biomolecules, physical interactions between neighbouring beads, and general education. Total costs per unit can be as low as ∼10 EUR while still producing a 0.6 pN/μm trap on multiple 1.5 μm beads.

Given the simplicity of fabrication, there is a basis for the rapid prototyping of progressively more complex microfluidic devices with micro-object trapping using bulk acoustic waves. For example, using multiple piezoelectric actuators and microchannel geometries may allow trapping and manipulation in all 3 dimensions. Combination with multiphysics approaches may rapidly increase functionality for small corresponding increase in device complexity (e.g. using light for local mechanical actuation to produce local acoustic fields). Acoustic forces are particularly suitable for operation in liquid environments, integration in optical microscopes and for (single) cell manipulation. We hope this simple and cheap device will enable easy access to a valuable scientific tool.

Funding D.F. and C.S.S. were supported by the Netherlands Organisation for Scientific Research (NWO) under NWO START-UP project No. 740.018.015. S.C. acknowledges an ERC starting grant (SIMPHONICS, No. 101041486). G.J.V. acknowledges support by the Dutch 4TU federation for the Plantenna project.

CRediT authorship contribution statement

Vi-hung Tsan: Methodology, Investigation, Software, Validation, Writing - original draft. **Daniel Fan:** Methodology, Supervision, Writing - original draft. **Sabina Caneva:** Methodology, Writing - review & editing. **Carlas S. Smith:** Conceptualization, Writing - review & editing, Funding acquisition. **Gerard J. Verbiest:** Conceptualization, Supervision, Funding acquisition, Writing - review & editing.

Declaration of Competing Interest

The authors declare the following financial interests/personal relationships which may be considered as potential competing interests: G.J. Verbiest reports financial support was provided by Dutch 4TU federation. S. Caneva reports financial support was provided by European Research Councel. D. Fan reports financial support was provided by Netherlands Organisation for Scientific Research. C.S. Smith reports financial support was provided by Netherlands Organisation for Scientific Research.

Acknowledgements

We would like to thank Murali Ghatkesar for discussions on acoustic impedance, Gurhan Ozkayar on microfluidic operation, and Dong Hoon Shin, Gideon Emmanuel, and Andres Hunt for help with glass cutting and drilling.

References

[1] Working principle of Acoustic Force Spectroscopy, LUMICKS,https://lumicks.com/knowledge/acousticforce-spectroscopy-and-z-movi-technology/ (visited on 08/25/2022).
[2] Microfluidic Acoustophoresis, uFluidix,https://www.ufluidix.com/microfluidics-research-reviews/microfluidicacoustophoresis/ (visited on 08/25/2022).
[3] A.-G. Niculescu, C. Chircov, A.C. Bîrcă, A.M. Grumezescu, Fabrication and Applications of Microfluidic Devices: A Review, Int. J. Mol. Sci. 22 (2021) 2011.
[4] V. Ortseifen, M. Viefhues, L. Wobbe, A. Grünberger, Microfluidics for Biotechnology: Bridging Gaps to Foster Microfluidic Applications, Front. Bioeng. Biotechnol. 8 (2020) 589074.
[5] G. Sitters, D. Kamsma, G. Thalhammer, M. Ritsch-Marte, E.J.G. Peterman, G.J.L. Wuite, Acoustic force spectroscopy, Nat. Methods 12 (2015) 47–50.
[6] A. Blázquez-Castro, Optical tweezers: phototoxicity and thermal stress in cells and biomolecules, Micromachines 10 (2019) 507.
[7] A. Ozcelik, J. Rufo, F. Guo, Y. Gu, P. Li, J. Lata, T.J. Huang, Acoustic tweezers for the life sciences, Nature Methods 15 (2018) 1021–1028.
[8] K.C. Neuman, A. Nagy, Single-molecule force spectroscopy: optical tweezers, magnetic tweezers and atomic force microscopy, Nature Methods 5 (2008) 491–505.
[9] A. Ashkin, J.M. Dziedzic, J.E. Bjorkholm, S. Chu, Observation of a single-beam gradient force optical trap for dielectric particles, Opt. Lett. 11 (1986) 288.
[10] A.R. Bausch, W. Möller, E. Sackmann, Measurement of Local Viscoelasticity and Forces in Living Cells by Magnetic Tweezers, Biophys. J. 76 (1999) 573–579.
[11] A. Karimi, S. Yazdi, A.M. Ardekani, Hydrodynamic mechanisms of cell and particle trapping in microfluidics, Biomicrofluidics 7 (2013) 021501.
[12] M.A. Gerspach, N. Mojarad, D. Sharma, T. Pfohl, Y. Ekinci, Soft electrostatic trapping in nanofluidics, Microsyst. Nanoeng. 3 (2017) 1–10.
[13] L. Meng, F. Cai, F. Li, W. Zhou, L. Niu, H. Zheng, Acoustic tweezers, J. Phys. D: Appl. Phys. 52 (2019) 273001.
[14] C. Bustamante, W. Cheng, Y.X. Mejia, Revisiting the central dogma one molecule at a time, Cell 144 (2011) 480–497.
[15] N.S. Goel, N. Richter-Dyn, Stochastic models in biology, Elsevier, 2016.
[16] M.A.B. Andrade, N. Pérez, J.C. Adamowski, Review of progress in acoustic levitation, Braz. J. Phys. 48 (2017) 190–213.
[17] G. Reinhart, J. Hoeppner, J. Zimmermann, Non-contact wafer handling using high-intensity ultrasonics, 2001 ieee/semi advanced semiconductor manufacturing conference (ieee cat no. 01ch37160), (IEEE, 2001, pp. 139–140.
[18] F. Guo, Z. Mao, Y. Chen, Z. Xie, J.P. Lata, P. Li, L. Ren, J. Liu, J. Yang, M. Dao, S. Suresh, and T.J. Huang, Three-dimensional manipulation of single cells using surface acoustic waves, Proc. Natl. Acad. Sci. 113, 1522–1527 (2016).
[19] M. Wu, A. Ozcelik, J. Rufo, Z. Wang, R. Fang, T. Jun Huang, Acoustofluidic separation of cells and particles, Microsyst. Nanoeng. 5 (2019) 1–18.
[20] J. van Mameren, P. Gross, G. Farge, P. Hooijman, M. Modesti, M. Falkenberg, G.J. Wuite, and E.J. Peterman, Unraveling the structure of dna during overstretching by using multicolor, single-molecule fluorescence imaging, Proc. Natl. Acad. Sci. 106, 18231–18236 (2009).
[21] S.B. Smith, Y. Cui, C. Bustamante, Overstretching b-dna: the elastic response of individual doublestranded and single-stranded dna molecules, Science 271 (1996) 795–799.
[22] Y. Zhou, M. Handley, G. Carles, A.R. Harvey, Advances in 3d single particle localization microscopy, APL Photon. 4 (2019) 060901.
[23] A. Lenshof, M. Evander, T. Laurell, J. Nilsson, Acoustofluidics 5: building microfluidic acoustic resonators, Lab Chip 12 (2012) 684–695.
[24] A. Ozcelik, J. Rufo, F. Guo, Y. Gu, P. Li, J. Lata, T.J. Huang, Acoustic tweezers for the life sciences, Nat. Methods 15 (2018) 1021–1028.
[25] A. Lenshof, M. Evander, T. Laurell, J. Nilsson, Acoustofluidics 5: Building microfluidic acoustic resonators, Lab Chip 12 (2012) 684.
[26] R. Krimholtz, D. Leedom, G. Matthaei, New equivalent circuits for elementary piezoelectric transducers, Electron. Lett. 6 (1970) 398.
[27] S.-I. Funano, N. Ota, Y. Tanaka, A simple and reversible glass-glass bonding method to construct a microfluidic device and its application for cell recovery, Lab Chip 21 (2021) 2244–2254.
[28] R.S. Figliola, D.E. Beasley, Theory and design for mechanical measurements, John Wiley & Sons, 2020.
[29] MatWeb, Overview of materials for epoxy adhesive,https://www.matweb.com/search/datasheettext.aspx?matguid=c1ec1ad603c74f628578663aaf44f261, Accessed: 2022-8-20.
[30] D. Blair and E. Dufresne, Particle location and tracking tutorial,https://site.physics.georgetown.edu/matlab/, Accessed: 2022-07-06.
[31] U. Kalwa, C. Legner, E. Wlezien, G. Tylka, and S. Pandey, New methods of removing debris and highthroughput counting of cyst nematode eggs extracted from field soil, PLOS ONE 14, edited by J. Zhang, e0223386 (2019).
[32] L. Huang, T. Liu, X. Yang, Y. Luo, Y. Rivenson, A. Ozcan, Holographic image reconstruction with phase recovery and autofocusing using recurrent neural networks, ACS Photon. 8 (2021) 1763–1774.
[33] G. Nootz, Fit 2d gaussian function to data,https://nl.mathworks.com/matlabcentral/fileexchange/37087-fit-2d-gaussian-function-to-data, Accessed: 2022-07-06.
[34] T. Baasch, I. Leibacher, J. Dual, Multibody dynamics in acoustophoresis, J. Acoust. Soc. Am. 141 (2017) 1664–1674.
[35] L.A. Carlucci, W.E. Thomas, Modification to axial tracking for mobile magnetic microspheres, Biophys. Rep. 1 (2021) 100031.
[36] J.P. Cnossen, D. Dulin, N. Dekker, An optimized software framework for real-time, high-throughput tracking of spherical beads, Rev. Sci. Instrum. 85 (2014) 103712.
[37] G. Pesce, G. Volpe, O.M. Maragó, P.H. Jones, S. Gigan, A. Sasso, G. Volpe, Step-by-step guide to the realization of advanced optical tweezers, JOSA B 32 (2015) B84–B98.

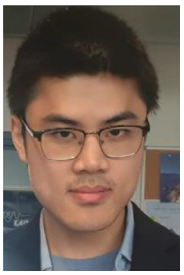

Vi-Hung Tsan received his BSc degree in Mechanical Engineering from the Delft University of Technology in 2018. He received the MSc degree in Mechanical Engineering as well as Systems and Control from the Delft University of Technology in 2022. During his studies he focused on high-tech engineering, opto-mechatronics systems design and control for high resolution imaging. For his master thesis, he worked on the design, fabrication and characterization of cost-effective ultrasound microfluidic acoustic tweezer. The main objective of this project is to present easy-to-build and low-cost acoustic tweezers available to anyone interested in conducting experiments with microparticles or micro-bead tethered DNA. By lowering the barrier to microparticle manipulation methods, He hopes that this will lead to accelerated breakthroughs.

Daniel Fan is a postdoctoral researcher at the Technical University of Delft, Netherlands, focusing on super-resolution microscopy, microfluidics, and 2-photon polymerization. He obtained a masters in micro and nano systems and a doctorate in materials science, both at ETH Zurich, Switzerland. Previously, he was an industrial electrical engineer working on electrical distribution and control systems. His research interests include optics, nanoscience, and lab-on-a-chip instrumentation. He recently obtained his seaplane pilot qualification and is currently based in Melbourne, Australia.

Dr Sabina Caneva is a tenure track assistant professor in Bionanoscience at TU Delft. She obtained a BSc and MSc in Materials Science from Oxford University (2012) and PhD in Engineering from the University of Cambridge (2016). Subsequently, she joined the Kavli Institute of Nanoscience in Delft as a postdoctoral researcher. Her work focused on molecular electronics and single-molecule biophysics, and she obtained a Marie Curie Fellowship to develop graphene tunnelling junctions for biosensing applications. Dr Caneva has been awarded a Delft Technology Fellowship to start her independent research group at the Department of Precision and Microsystems Engineering, TU Delft, in May 2020. Her group develops nanoelectromechanical systems for molecular diagnostics using a combination of nanopore measurements, fluorescence imaging and acoustofluidics.

Dr. Carlas S. Smith is an associate professor in the Delft Center for Systems and Control at Delft University of Technology. His research transcends the classic boundaries between biology and engineering to visualize single molecules in living cells. For this purpose, he combines advanced control strategies, algorithm development, and computational microscopy technology.

Gerard J. Verbiest is a tenure track assistant professor in Mechanical Engineering at TU Delft. He obtained his M.Sc. degree in theoretical physics (cum laude, 2009), and a PhD in experimental physics (2013) from Leiden University. His doctorate work focused on the application of ultrasound at MHz frequencies in atomic force microscopes to enable subsurface atomic force microscopy. He then worked as postdoctoral researcher at the RWTH Aachen in Germany between 2013 and 2018 on graphene mechanics and dynamics. Since August 2018, Gerard works as assistant professor at the Delft University of Technology. His work focusses on nanoscale acoustics with applications in atomic force microscopes, graphene and other two-dimensional materials, and plant physiology.